Detecting and Reducing the Effects of Postseismic Deformation in Observed GPS Time Series Using a Hybrid Forward/Inverse Method in Southern California

Katherine Guns[1] & Richard Bennett[1]

[1]University of Arizona, Department of Geosciences, 1040 E. 4th Street, Tucson, AZ , 85721

Contact: Katherine Guns (kguns@email.arizona.edu)

Motivation

+ Viscoelastic postseismic deformation caused by large magnitude earthquakes can last for years to decades after the main event.
+ High precision GPS instruments in southern California may still be observing postseismic deformation from historical and recent earthquakes in the southwest U.S.
+ This type of long-term deformation can bias both crustal GPS velocities and geodetic-based fault slip rate estimates, but can be difficult to detect in GPS time series.

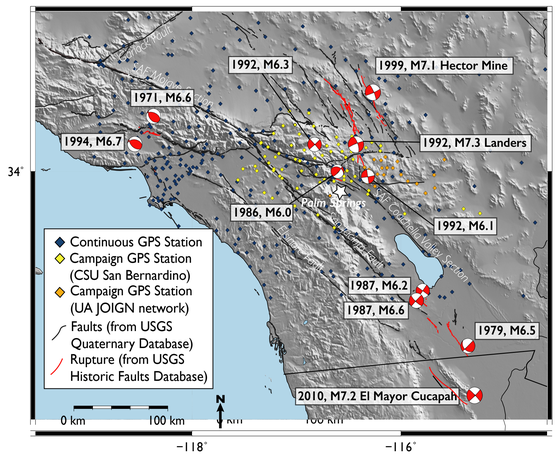

Figure 1. The extent of networks of continuous and campaign style GPS stations in southern California used in this study, in addition to all M6.0+ earthquakes that have occurred in the last 50 years (excluding the recent M7.1 Ridgecrest event which is off the map). Campaign GPS data comes from the JOIGN network (UA) and the San Bernardino network run by Sally McGill (CSUSB).

Method

GOAL: To identify and reduce the effect of ongoing postseismic viscoelastic relaxation on GPS time series

(1) FORWARD MODELING

Choose Earth elastic and viscosity structure — **Figure 2** — *Broermann (2017)*

↓

Calculate Green's Functions with PSGRN software — *Wang et al. (2006)*

↓

Organize finite fault models for all 217 earthquake events — **Figure 3** — *Wang et al. (2009) SRCMOD Database USGS Earthquake Catalog*

↓

Calculate model surface displacements for each event at locations of network GPS stations using PSCMP software — *Wang et al. (2006)*

↓

Determine which events measurably impact our GPS time series (yr. 2000-2018) — **Figure 4**

↓

Subtract those events' postseismic displacements from modern time series — **Figure 5**

(2) INVERSE MODELING

Estimate velocities from forward model **postseismic reduced** time series

Estimate velocities from **observed, un-reduced** time series — **Figure 5** **Figure 7** — *TSVIEW / TSFIT & Hector software*

↓

Estimate **logarithmic postseismic terms** for recent conspicuous events from **both sets**, to assess success of forward model — **Figure 6** — *TSVIEW / TSFIT & Hector software*

Method

(1) Forward modeling earthquake displacements

+ PSGRN + Earth Model

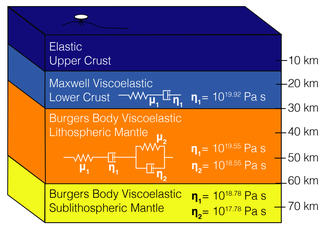

Figure 2. Our chosen viscoelastic Earth structure from Broermann (2017). This is a layered, laterally homogenous Earth model from which all Green's functions are calculated in PSGRN (Wang et al., 2006).

+ 217 ≥M6.0 Earthquakes modeled in PSCMP

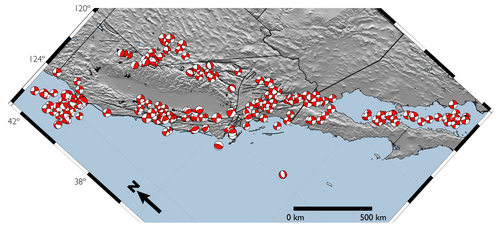

Figure 3. Locations of 216 ≥M6.0 earthquakes since 1800, for which we calculated surface displacements caused by viscoelastic postseismic deformation (one earthquake not shown as it is off map in Sonora, MX). These earthquakes and their rupture characteristics come from the Wang et al. (2009) catalog, and the USGS Earthquake Catalog when not present in the SRCMOD database.

+ 12 Earthquakes with ongoing displacements

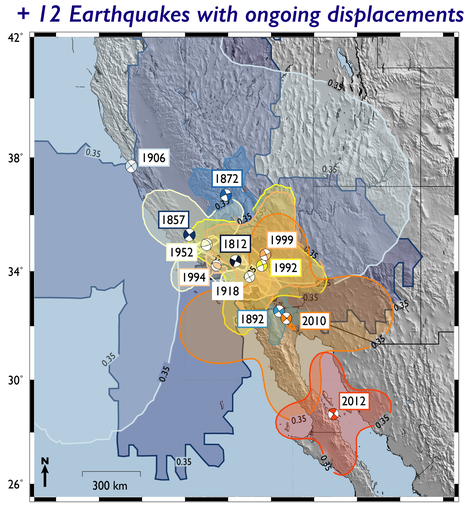

Figure 4. Of all 217 earthquakes modeled using PSCMP and our chosen earth structure, 12 events still exhibited measurable ongoing year-cumulative surface displacements ≥0.35 mm in any year 2000-2018 for any station in our southern CA network. This figure illustrates the 0.35 mm contour of cumulative displacements in 2018 for each event, where the areas inside the contour had cumulative displacements >0.35 mm.

(2) Inverse Modeling: Reduced Time Series & Estimating Logarithmic Terms

+ Reducing Time Series & Estimating Velocities

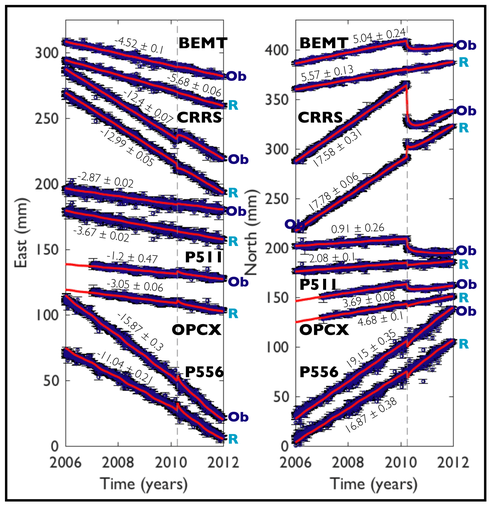

Figure 5. (above) Stacked time series plot of a selection of stations zoomed in to the 2010 El Mayor-Cucapah earthquake (vertical dashed grey line), comparing observed time series (at top of every pair, labeled with "Ob" at right) and forward model postseismic reduced time series (at bottom of every pair, labeled with "R" at right) that have been corrected for the 12 earthquakes shown in **Figure 4.** Stations BEMT, OPCX, and P511 show examples of successful reduction of postseismic displacements, while station CRRS shows an example of a reduction in which most of the postseismic displacements have been removed, but the coseismic jump has been overcorrected. Station P556 shows an example of the case in which our postseismic reduction have little effect on the 2010 displacements.

$$\sigma^2 \text{ Reduction} = \frac{\sqrt{A' \cdot V^{-1} \cdot A} - \sqrt{B' \cdot W^{-1} \cdot B}}{\sqrt{A' \cdot V^{-1} \cdot A}}$$

+ Estimating Log Terms for 2010 El Mayor-Cucapah

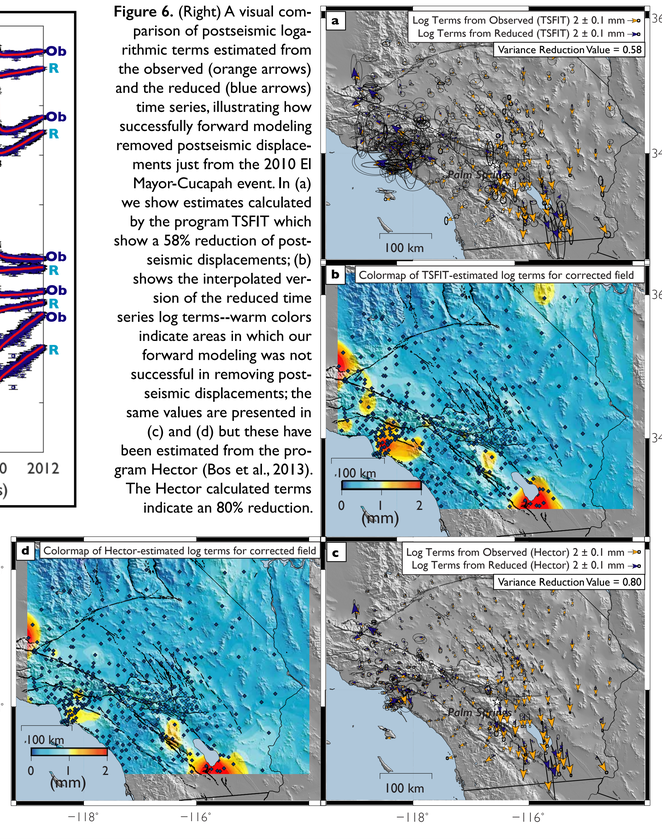

Figure 6. (Right) A visual comparison of postseismic logarithmic terms estimated from the observed (orange arrows) and the reduced (blue arrows) time series, illustrating how successfully forward modeling removed postseismic displacements just from the 2010 El Mayor-Cucapah event. In (a) we show estimates calculated by the program TSFIT which show a 58% reduction of postseismic displacements; (b) shows the interpolated version of the reduced time series log terms--warm colors indicate areas in which our forward modeling was not successful in removing postseismic displacements; the same values are presented in (c) and (d) but these have been estimated from the program Hector (Bos et al., 2013). The Hector calculated terms indicate an 80% reduction.

Results

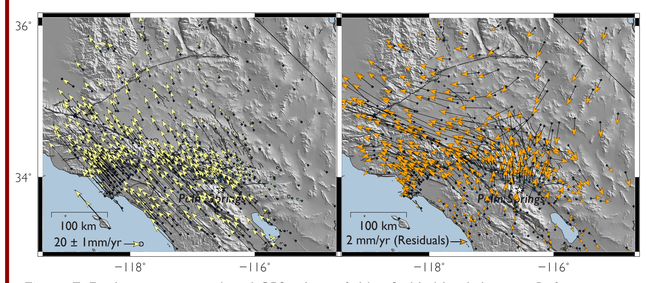

Figure 7. Final postseismic-reduced GPS velocity field in Stable North America Reference Frame (NAM08) (left, yellow) and the residual velocity field (observed velocities - reduced velocities) (right) showing the directions and magnitudes of the removed postseismic biases at each station (note factor of ten difference between scales). Error ellipses are 95% confidence interval.

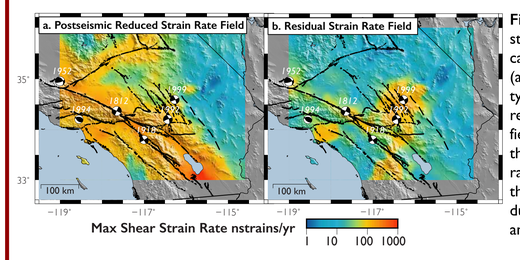

Figure 8. Shear strain rate maps calculated from the (a) reduced velocity field and (b) the residual velocity field. This illustrates the high strain rates in the ECSZ that have been reduced through this analysis.

Implications for fault slip rates?

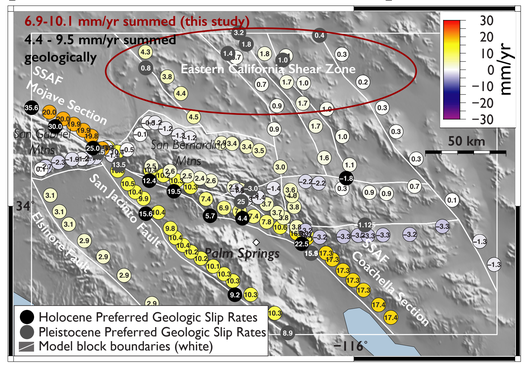

Figure 9. Preliminary slip rate estimates from inverting our postseismic reduced velocity field using the fault block geometry outlined in white using tDEFNODE (McCaffrey, 2005). The most intriguing result is that our geodetic-based fault slip rate values match or nearly match those in the Eastern CA Shear Zone (compare to grey circles with preferred geologic slip rates).

Summary

- We identify **12 historical and recent earthquakes** that have greater than 0.35 mm/yr of summed cumulative displacements in any year 2000-2018, indicating **measureable ongoing displacements**.
- We successfully **reduce postseismic deformation** for the 2010 El Mayor-Cucapah earthquake **by up to 80%** (58% measured through values from TSFIT and 80% measured throught values from Hector) by removing displacements from these 12 earthquakes from modern time series
- Preliminary block modeling using our postseismic reduced velocity field indicates **possible agreement between geologic and geodetic slip rates** in the Eastern California Shear Zone

References

+ Bos, M.S., Fernandes, R.M.S., Williams, S.D.P., & Bastos, L. (2013). Fast Error Analysis of Continuous GNSS Observations with Missing Data. J. Geod., 87(4), 351-360.
+ Broermann, James. (2017). Appendix B:Time-independent and time-varying surface velocity field for the Colorado Plateau and adjacent Basin and Range inferred from viscoelastic modeling, in Alignment of post-Atlantic-rifting Volcanic Features on the Guinea Plateau, West Africa, and Present-Day Deformation in the Southwest United States from GPS Geodesy. PhD Dissertation, University of Arizona.
+ Cardozo, N. & Allmendinger, R.W. (2009). SSPX: A program to compute strain from displacement/velocity data. Comp. & Geos. 35, 1343-1357.
+ Herring, T.A., King, R.W., Floyd M.A., & McClusky, S.C. (2018). Introduction to GAMIT/GLOBK, Release 10.7, GAMIT/GLOBK Documentation, http://geoweb.mit.edu/gg/docs.php
+McCaffrey, Robert. (2005). Block kinematics of the Pacific-North America plate boundary in the southwestern United States from inversion of GPS, seismological, and geologic data, JGR, 110(B07401).
+ Wang, Q., Jackson, D.D., & Kagan, Y.Y. (2009). California Earthquakes, 1800-2007: A Unified Catalog with Moment Magnitudes, Uncertainties, and Focal Mechanisms. SRL, 80(3), 446-457.
+ Wang, R., Lorenzo-Martin, F., & Roth, F. (2006). PSGRN/PSCMP—a new code for calculating co- and post-seismic deformation, geoid and gravity changes based on the viscoelastic-gravitational dislocation theory. Comp. & Geos., 32, 527-541.
+Wessel, P., Smith, W.H.F., Scharroo, R., Luis, J., & Wobbe, F. (2013). Generic Mapping Tools: Improved Version Released. EOS Transactions, American Geophysical Union, 94(45), 409-420.

Acknowledgments

We would like to thank Professor Sally McGill for her willingness to share her campaign data from the San Bernardino Mtns. with us before it was publicly archived at UNAVCO. We would also like to thank the University of Arizona Dr. H. Wesley Peirce and Maxine W. Peirce Scholarship, the GSA John T. and Carol G. McGill Research Award and the GSA ExxonMobil Award for helping to fund this work.

SCEC 2019: Poster #197, Award #17161